Rapid Communications

Quasistatic internal magnetic field detected in the pseudogap phase of $Bi_{2+x}Sr_{2-x}CaCu_2O_{8+\delta}$ by muon spin relaxation

A. Pal,[1] S. R. Dunsiger,[1] K. Akintola,[1] A. C. Y. Fang,[1] A. Elhosary,[1] M. Ishikado,[2] H. Eisaki,[3] and J. E. Sonier[1,4]

[1]*Department of Physics, Simon Fraser University, Burnaby, British Columbia, Canada V5A 1S6*

[2]*Neutron Science and Technology Center, Comprehensive Research Organization for Science and Society (CROSS), Tokai, Naka, Ibaraki 319-1106, Japan*

[3]*National Institute of Advanced Industrial Science and Technology, Tsukuba, Ibaraki 305-8568, Japan*

[4]*Canadian Institute for Advanced Research (CIFAR), Toronto, Ontario, Canada M5G 1Z8*

(Received 4 July 2017; revised manuscript received 22 September 2017; published 8 February 2018)

We report muon spin relaxation (μSR) measurements of optimally doped and overdoped $Bi_{2+x}Sr_{2-x}CaCu_2O_{8+\delta}$ single crystals that reveal the presence of a weak temperature-dependent quasistatic internal magnetic field of electronic origin in the superconducting and pseudogap (PG) phases. In both samples the internal magnetic field persists up to 160 K, but muon diffusion prevents following the evolution of the field to higher temperatures. We consider the evidence from our measurements in support of PG order parameter candidates, namely, electronic loop currents and magnetoelectric quadrupoles.

DOI: 10.1103/PhysRevB.97.060502

In high transition temperature (T_c) cuprate superconductors, the origin of the pseudogap (PG), associated with a loss of low-energy electronic spectral weight above T_c, is an enduring mystery. However, it is widely believed to be a manifestation of a thermodynamic transition to a phase which breaks various symmetries [1]. One longstanding idea is that electronic loop-current order with translation symmetry forms in the PG phase [2–4]. The apparent detection of an ubiquitous intraunit cell (IUC) magnetic order in various cuprate families by polarized neutron diffraction (PND) [5–14] lends support to this proposal. The existence of magnetic order in the PG phase is supported by the observation of the Kerr effect in $YBa_2Cu_3O_y$ (Y123) [15,16]. Motivated by these results and other loop-current order predictions [1], there have been numerous unsuccessful attempts to detect intrinsic magnetic order in the PG phase of high-T_c cuprates by zero-field (ZF) muon spin rotation (μSR) [17–22], and nuclear magnetic resonance (NMR) [23–26].

At odds with the above-mentioned neutron results is a recent PND experiment which failed to detect magnetic order in the PG phase of high-quality underdoped Y123 single crystals [27]. It has since been argued that this new neutron experiment is not sensitive enough to detect the IUC magnetic order [28], particularly if the correlation length associated with the broken symmetry state is finite. Thus, there is uncertainty as to the origin of the PND signal. It has been proposed that the PND experiments do not directly detect magnetic dipolar ordering, but rather quasistatic ordering of magnetoelectric multipoles [29]. In this scenario, internal magnetic fields generated by the magnetoelectric quadrupole ordering are estimated to be below the detection limit of NMR, but potentially detectable by ZF-μSR [30]. This highlights the need to explore this phenomenon with complementary techniques.

The ZF-μSR method is sensitive to weak internal magnetic fields originating from magnetic order or randomly oriented magnetic dipoles. Originally, theory [2] predicted an oscillatory ZF-μSR signal indicative of static IUC magnetic order, which has never been observed [31]. This has led to speculation that the IUC magnetic order resides in fast fluctuating domains [4], which may cause only weak or no relaxation of the ZF-μSR signal [22,32]. In hindsight, Y123 is nonideal for ZF-μSR investigations of IUC magnetic order or magnetoelectric quadrupole ordering, because a weak magnetic component associated with either phenomena cannot be disentangled from other contributions to the ZF-μSR signal. In particular, μSR studies of Y123 [17,18,20,32] must account for the known effects of charge-density-wave (CDW) order in the CuO chains, a potential unbuckling of the CuO_2 layers, and muon diffusion [18,33,34], as well as magnetic correlations due to oxygen vacancies in the CuO chains [35]. Although μSR studies of $La_{2-x}Sr_xCuO_4$ (La214) [19,21] are limited only by muon diffusion, the failure to detect PG magnetic order in this compound is not surprising given that neutrons have thus far only detected short-range, two-dimensional IUC magnetic order in La214 far below the PG temperature (T^*) [8].

We report zero-field (ZF) and longitudinal-field (LF) μSR measurements on a more promising system, namely, optimally doped and overdoped $Bi_{2+x}Sr_{2-x}CaCu_2O_{8+\delta}$ (Bi2212) single crystals with $T_c = 91$ K (OP91) and $T_c = 80$ K (OD80), respectively. Details on the sample preparation are provided in the Supplemental Material [36], while the μSR technique is described elsewhere [37]. All μSR asymmetry spectra were recorded with the initial muon spin polarization $\mathbf{P}(0)$ (and LF) parallel to the $\hat{c}$ axis. The spectra are of the form $A(t) = a_0 G_z(t)$, where a_0 is the initial asymmetry and $G_z(t)$ describes the time evolution of the muon spin polarization due to the local magnetic fields sensed by the implanted muon ensemble.

ZF-μSR. Figure 1 shows representative ZF-μSR asymmetry spectra recorded for the OP91 sample. As shown in Fig. 1(a), the ZF-μSR spectra below 160 K are well described by the product of an exponential relaxation function and

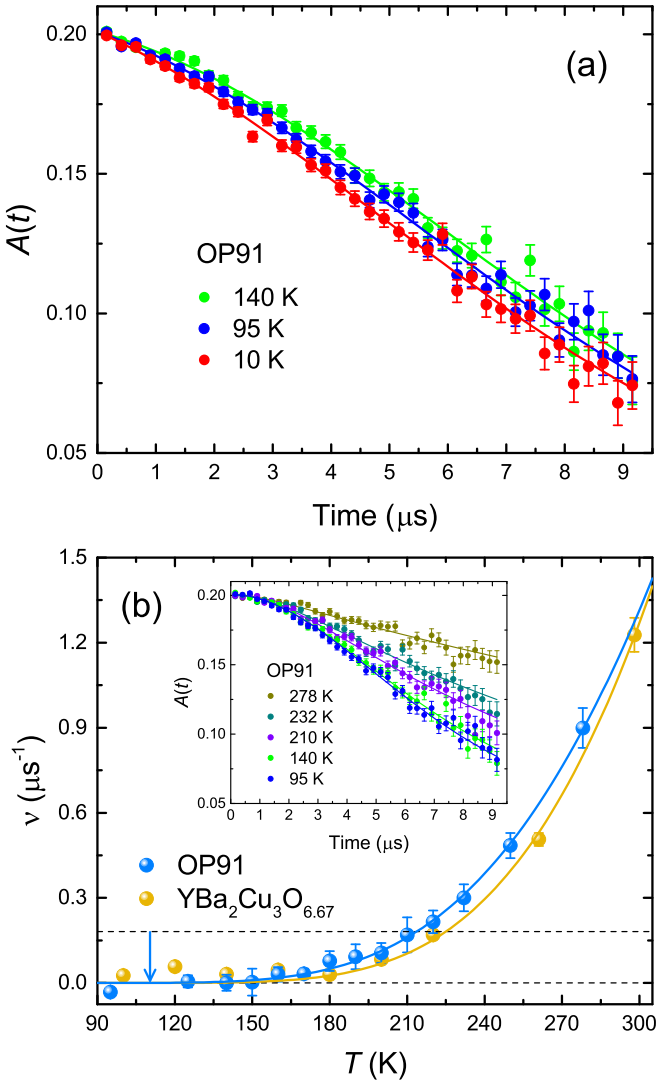

FIG. 1. (a) Representative ZF-μSR spectra below 160 K with fits to Eq. (1). (b) Temperature dependence of the muon hop rate ν in the OP91 sample together with similar data for underdoped Y123 [18]. For the purpose of comparison, the OP91 data are shifted downward by 0.181 μs^{-1}. The solid curves are fits to an Arrhenius equation $\nu = A\exp(-E_0/k_BT)$, which yield an activation energy of $E_0 = 127(5)$ meV for OP91 and $E_0 = 151(9)$ meV for underdoped Y123. The inset shows representative ZF-μSR spectra for the OP91 sample and fits to $G_{KT}(\Delta,\nu,t)$, with Δ a common fit parameter.

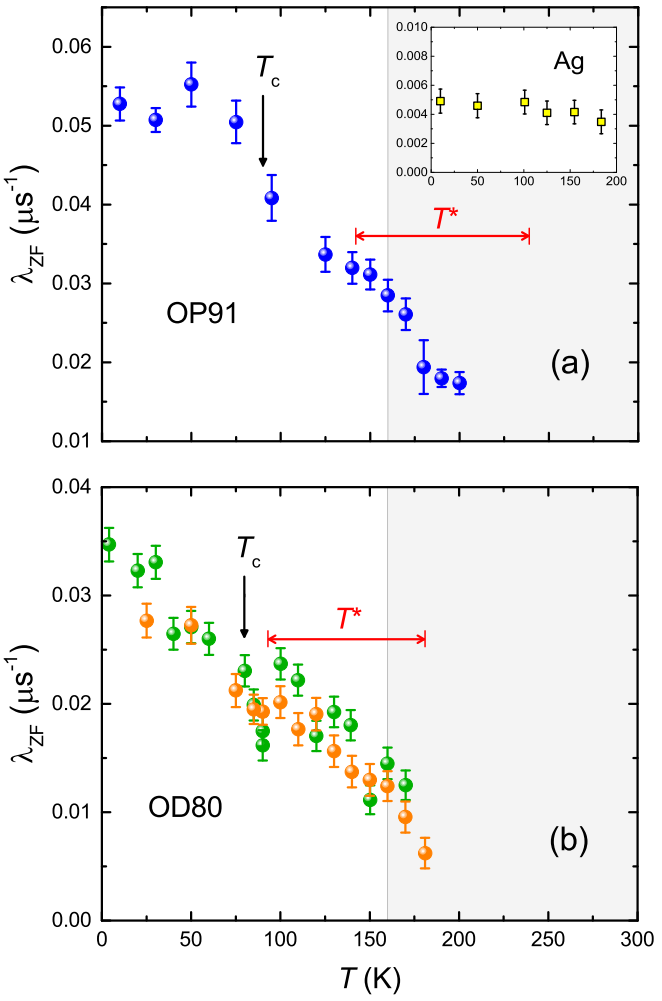

FIG. 2. Temperature dependence of the exponential ZF relaxation rate λ_{ZF} in the (a) OP91 and (b) OD80 samples. The two data sets for the OD80 sample are from measurements performed during different beam periods. The range of values for T^* is from Ref. [39]. The inset in (a) shows λ_{ZF} measured separately in a 5.45 × 6.54 × 0.25 mm sample of 99.998% pure Ag foil. The values of λ_{ZF} for Ag come from fits to Eq. (1) with $\Delta = 0$.

a T-independent static Gaussian ZF Kubo-Toyabe function [37] intended to account for a nuclear-dipolar contribution. Specifically,

$$G_z(t) = G_{KT}(\Delta,t)\exp(-\lambda_{ZF}t), \quad (1)$$

where Δ^2 is the second moment of the internal static magnetic field distribution, assumed to be Gaussian. Global fits of the ZF-μSR spectra as a function of temperature with Δ as a common parameter yield $\Delta = 0.0958(6)$ μs^{-1} and $\Delta = 0.095(1)$ μs^{-1} for the OD80 and OP91 samples, respectively. Figure 2 shows the temperature dependence of the relaxation rate λ_{ZF}. For comparison, the inset of Fig. 2(a) shows λ_{ZF} vs T measured in a sample of 99.998% pure Ag comparable in size to the Bi2212 samples. The ZF relaxation rate in Ag is solely due to weak nuclear dipole fields, and is essentially negligible. The results on Ag show that any temperature dependence in λ_{ZF} between 184 and 10 K is less than 0.0014 μs^{-1}. On the other hand, λ_{ZF} in the Bi2212 samples exhibits a significant decrease with increasing T.

Above 200 K, Eq. (1) no longer adequately describes the data. Specifically, the slower relaxation rate observed at the highest temperatures in the inset of Fig. 1(b) is due to muon diffusion. To show this is the case, the spectra at $T \geqslant 95$ K were fit to the nonanalytic strong-collision dynamic Gaussian Kubo-Toyabe relaxation function $G_{KT}(\Delta,\nu,t)$ [38], where ν is the muon hop rate, or, equivalently, the average rate at which there are changes in the local magnetic field sensed by the muon. The temperature dependence of the fitted ν with a zero offset correction is shown in Fig. 1(a), together with earlier results for underdoped Y123 [18]. The zero offset of ν suggests the magnetic field distribution in Bi2212 is not as close to a

Gaussian as in Y123. Such deviations from a Gaussian form are to be anticipated, having been observed in La214 [21], and can be quantitatively accounted for if the muon site(s) and electric field gradients in the material are known. With the zero offset correction, the hop rate in Bi2212 obeys an Arrhenius relationship similar to Y123. In both compounds, ν increases above $T \sim 160$ K, indicating a similar onset temperature for muon diffusion. In cuprates the muon is known to form an O-H like bond with an oxygen ion. The results here imply that the thermal energy required to break the O-μ bond in Bi2212 is comparable to Y123. Unfortunately, muon diffusion masks clear evidence of PG magnetic order above 160 K. However, at lower temperatures, the behavior reflects a change in the linewidth of the internal magnetic field distribution sensed by the muon ensemble, which *cannot* be explained in terms of muon diffusion alone. This is our main finding.

The values of T^* for Bi2212 are ill defined. The temperature ranges for T^* indicated in Fig. 2 come from a compilation of values measured by different techniques [39]. Because the range of experimental values for T^* extend above 160 K, we cannot say whether there is a spontaneous ZF relaxation appearing at the PG onset.

LF-μSR. To determine whether the local magnetic field detected in the PG region is static or fluctuating, we performed LF-μSR measurements on each sample just above T_c. Figure 3(a) shows LF-μSR asymmetry spectra for the OD80 sample with fits assuming the relaxation function

$$G_z(t) = G_{\rm KT}(B_{\rm LF}, \Delta, t)\exp(-\lambda_{\rm LF} t). \quad (2)$$

Here, $G_{\rm KT}(B_{\rm LF}, \Delta, t)$ is an extension of $G_{\rm KT}(\Delta, t)$ to the LF case [37], which accounts for the addition of the applied field $B_{\rm LF}$ to the local internal nuclear dipole fields. The external field does not reorient the nuclear dipoles, and hence Δ was fixed to the values determined by ZF-μSR below Eq. (1). The field dependence of the residual exponential relaxation rate $\lambda_{\rm LF}$ [Fig. 3(b)] is well described by the Redfield theory [38],

$$\lambda_{\rm LF} = \frac{\gamma_\mu^2 \langle B_\mu^2 \rangle \tau}{1 + (\gamma_\mu B_{\rm LF} \tau)^2}, \quad (3)$$

where $\gamma_\mu/2\pi$ is the muon gyromagnetic ratio, $\langle B_\mu^2 \rangle$ is the mean of the square of the fluctuating transverse field components, and $1/\tau$ is the characteristic fluctuation rate of the local fields B_μ. Fits to this equation yield $\langle B_\mu^2 \rangle^{1/2} = 1.4(2)$ G and $1/\tau = 0.7(1)$ MHz for the OP91 sample, and $\langle B_\mu^2 \rangle^{1/2} = 1.3(3)$ G and $1/\tau = 0.6(2)$ MHz for the OD80 sample. Thus the residual local internal magnetic field sensed by the muon is quasistatic and on the order of the resultant field of the nuclear dipoles. In ortho-II Y123, NMR measurements place upper limits of 4 and 0.3 G for any magnetic field fluctuating slower than ~0.01 MHz at the planar and apical oxygen sites, respectively [26]. A similar upper bound for static local fields at the apical oxygen site has been deduced from NMR on $HgBa_2CuO_{4+\delta}$ (Hg1201) [25]. Hence, the weak quasistatic fields detected here in Bi2212 are likely fluctuating too fast to be detected by NMR.

We now systematically discuss explanations for the observed muon spin relaxation. Below 160 K where the implanted muon is immobile, the T-dependent $\lambda_{\rm ZF}$ may originate from a continuous change in the nuclear dipole contribution or be caused by magnetic dipole moments of an electronic origin.

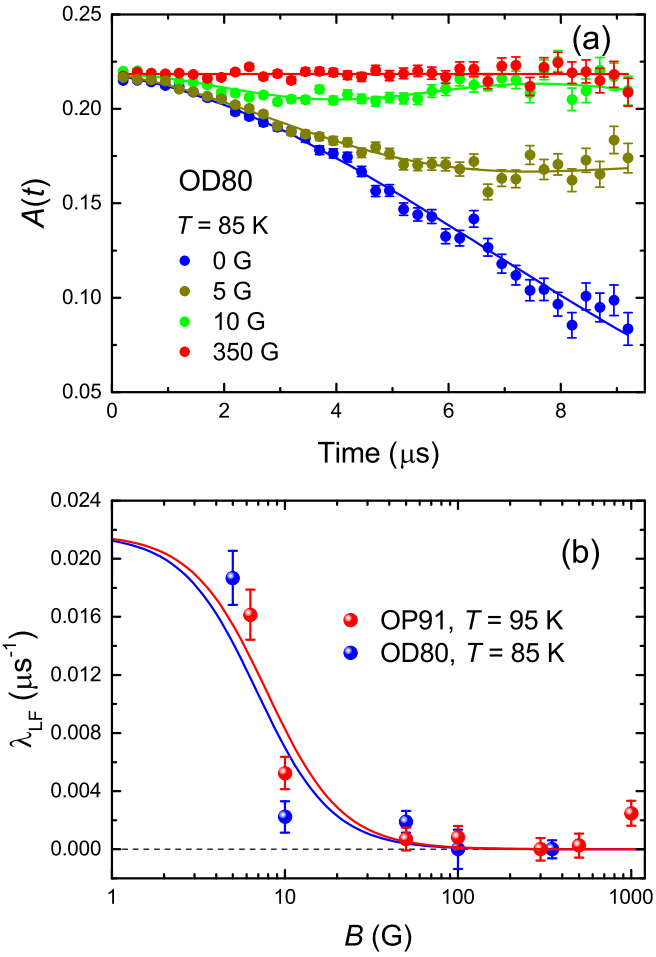

FIG. 3. (a) Representative LF-μSR asymmetry spectra recorded on the OD80 sample at $T = 85$ K. The curves are fits to Eq. (2). (b) Dependence of the LF exponential relaxation rate $\lambda_{\rm LF}$ on the applied magnetic field. The solid curves are fits to Eq. (3). The relaxation rates above 100 G are at the sensitivity limit of μSR and may be compared with the values of $\lambda_{\rm ZF}$ in Ag.

The former may result from structural changes that modify the distance between the muon and nuclear spins, as well as the direction of the maximal local electric field gradient (EFG) that defines the quantization axis for the nuclear spins. A T-dependent electric quadrupolar interaction of the nuclei with the local EFG can also result from a gradual development of charge inhomogeneity or charge order. While ^{17}O NMR measurements on overdoped Bi2212 ($T_c = 82$ K) demonstrate an inhomogeneous distribution of local EFG at the O(1) sites in the CuO_2 plane, this does not evolve with temperature [40]. X-ray scattering measurements on underdoped Bi2212 show the development of CDW order within the PG phase [41], persisting as weak dynamic CDW correlations near T^* [42]. Indeed, short-range CDW order has been identified in recent years to be ubiquitous in cuprates [43]. However, the CDW correlations are most pronounced in the underdoped regime and significantly weaken or fade away near optimal doping. Moreover, in contrast to $\lambda_{\rm ZF}$ (Fig. 2), the CDW correlations are suppressed below T_c. Hence CDW correlations do not seem to explain the T-dependent ZF relaxation rate observed below 160 K.

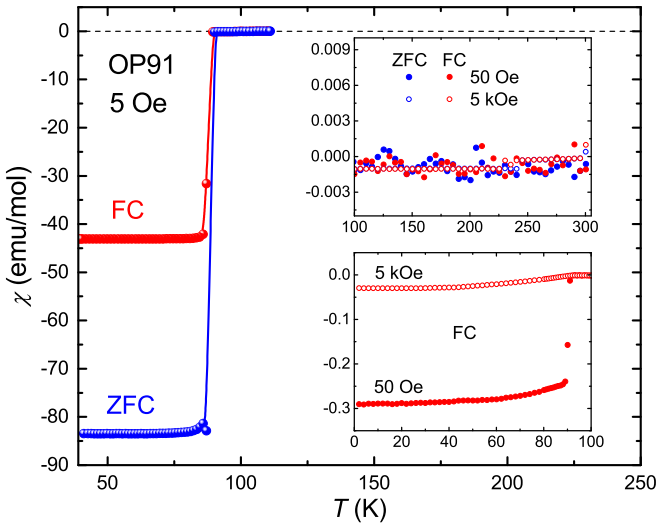

FIG. 4. Temperature dependence of the bulk magnetic susceptibility for the OP91 sample measured in an applied magnetic field of $H = 5$ Oe under field-cooled (FC) and zero-field-cooled (ZFC) conditions. The insets show similar measurements above and below T_c at $H = 50$ and 5 kOe.

Another potential source of the ZF relaxation is dilute magnetic impurities. Dilute remnants of the underdoped phase containing Cu spin correlations fluctuating slow enough to be detectable on the μSR time scale are unlikely to be present near and above optimal doping. Bulk magnetization measurements down to 2 K show no evidence of a magnetic impurity or secondary phase. As shown in Fig. 4, the normal-state magnetic susceptibility of the OP91 sample measured up to 300 K exhibits no low-T upturn indicative of a paramagnetic impurity.

A previous weak LF-μSR study of overdoped polycrystalline samples of $Bi_2Sr_2Ca_{1-x}Y_xCu_2O_{8+\delta}$ revealed a small increasing relaxation rate below $T \sim 135$ K at 20 G in a $T_c = 81$ K sample [44]. While attributed to an inhomogeneous distribution of internal magnetic field generated by superconducting (SC) domains, the frequency scale for SC fluctuations above T_c ($10^{10}-10^{14}$ Hz) established by other methods [45–47] is too high to produce an observable LF relaxation. Inserting $\langle B_\mu^2\rangle^{1/2} \leqslant 20$ G and $1/\tau = 10^{10}$ Hz in Eq. (3) yields $\lambda_{\rm LF} \leqslant 3 \times 10^{-4}$ μs^{-1}, which is far smaller than the LF relaxation rates reported in Ref. [44] and well below the reliable detection limit.

The IUC magnetic order in Bi2212 inferred by neutrons is characterized by a pair of staggered magnetic moments in the CuO_2 unit cell predominantly perpendicular to the CuO_2 plane and displaced from a Cu atom along the [1,1,0] direction, with an ordered magnetic moment of $\sim 0.1\mu_B$ [12]. While the precise *muon* site in Bi2212 is undetermined, the muon is expected to reside near an O atom. Calculations of the magnetic dipolar field generated by *static* IUC magnetic order at the *oxygen* sites in the CuO_2, SrO, and BiO planes yield 3.1, 116, and 1.4 G, respectively. Two of these values are on the order of the magnitude of the quasistatic internal field just above T_c estimated from the LF-μSR data. However, this does not exclude the possibility of magnetic order fluctuating too fast to be detectable on the μSR time scale, or, equivalently, $\lambda_{\rm ZF} = \gamma_\mu^2\langle B_\mu^2\rangle\tau \lesssim 0.001$ μs^{-1}. With this said, the detected field is close to the calculated size of the internal magnetic fields generated by *quasistatic* magnetoelectric quadrupolar ordering—estimated to be $\sim$0.3 G at the oxygen sites in Hg1201 [30] and potentially larger at the muon site(s) in Bi2212.

In summary, we have detected a weak T-dependent *quasistatic* internal magnetic field in the SC and PG phases of Bi2212, seemingly of electronic and intrinsic origin. While consistent with a static version of the IUC magnetic order inferred from neutron measurements, this interpretation is difficult to reconcile with μSR studies of other cuprates. Our findings offer some support for a theory ascribing the primary order parameter in the PG phase to quasistatic magnetoelectric quadrupoles.

We thank Marc-Henri Julien and Michael Fechner for insightful comments, and the TRIUMF staff for technical assistance. Sample preparation was performed at the CROSS user laboratories. The present work was partially supported by Canadian Institute for Advanced Research (CIFAR), Natural Sciences and Engineering Research Council of Canada (NSERC; PIN:146772), and Japan Society for the Promotion of Science (JSPS) Grants-in-Aid for Scientific Research (KAKENHI) Grant No. JP15K17712.

[1] S. Chakravarty, R. B. Laughlin, D. K. Morr, and C. Nayak, Phys. Rev. B **63**, 094503 (2001).
[2] C. M. Varma, Phys. Rev. B **55**, 14554 (1997).
[3] C. M. Varma, Phys. Rev. B **73**, 155113 (2006).
[4] C. M. Varma, J. Phys.: Condens. Matter **26**, 505701 (2014).
[5] B. Fauqué, Y. Sidis, V. Hinkov, S. Pailhès, C. T. Lin, X. Chaud, and P. Bourges, Phys. Rev. Lett. **96**, 197001 (2006).
[6] H. A. Mook, Y. Sidis, B. Fauqué, V. Balédent, and P. Bourges, Phys. Rev. B **78**, 020506(R) (2008).
[7] Y. Li, V. Balédent, N. Barišić, Y. Cho, B. Fauqué, Y. Sidis, G. Yu, X. Zhao, P. Bourges, and M. Greven, Nature (London) **455**, 372 (2008).
[8] V. Balédent, B. Fauqué, Y. Sidis, N. B. Christensen, S. Pailhès, K. Conder, E. Pomjakushina, J. Mesot, and P. Bourges, Phys. Rev. Lett. **105**, 027004 (2010).
[9] V. Balédent, D. Haug, Y. Sidis, V. Hinkov, C. T. Lin, and P. Bourges, Phys. Rev. B **83**, 104504 (2011).
[10] Y. Li, V. Balédent, N. Barišić, Y. C. Cho, Y. Sidis, G. Yu, X. Zhao, P. Bourges, and M. Greven, Phys. Rev. B **84**, 224508 (2011).
[11] S. De Almeida-Didry, Y. Sidis, V. Balédent, F. Giovannelli, I. Monot-Laffez, and P. Bourges Phys. Rev. B **86**, 020504(R) (2012).
[12] L. Mangin-Thro, Y. Sidis, P. Bourges, S. De Almeida-Didry, F. Giovannelli, and I. Laffez-Monot, Phys. Rev. B **89**, 094523 (2014).

[13] L. Mangin-Thro, Y. Sidis, A. Wildes, and P. Bourges, Nat. Commun. **6**, 7705 (2015).

[14] L. Mangin-Thro, Y. Li, Y. Sidis, and P. Bourges, Phys. Rev. Lett. **118**, 097003 (2017).

[15] J. Xia, E. Schemm, G. Deutscher, S. A. Kivelson, D. A. Bonn, W. N. Hardy, R. Liang, W. Siemons, G. Koster, M. M. Fejer, and A. Kapitulnik, Phys. Rev. Lett. **100**, 127002 (2008).

[16] A. Kapitulnik, J. Xia, E. Schemm, and A. Palevski, New J. Phys. **11**, 055060 (2009).

[17] J. E. Sonier, J. H. Brewer, R. F. Kiefl, R. I. Miller, G. D. Morris, C. E. Stronach, J. S. Gardner, S. R. Dunsiger, D. A. Bonn, W. N. Hardy, R. Liang, and R. H. Heffner, Science **292**, 1692 (2001).

[18] J. E. Sonier, J. H. Brewer, R. F. Kiefl, R. H. Heffner, K. F. Poon, S. L. Stubbs, G. D. Morris, R. I. Miller, W. N. Hardy, R. Liang, D. A. Bonn, J. S. Gardner, C. E. Stronach, and N. J. Curro, Phys. Rev. B **66**, 134501 (2002).

[19] G. J. MacDougall, A. A. Aczel, J. P. Carlo, T. Ito, J. Rodriguez, P. L. Russo, Y. J. Uemura, S. Wakimoto, and G. M. Luke, Phys. Rev. Lett. **101**, 017001 (2008).

[20] J. E. Sonier, V. Pacradouni, S. A. Sabok-Sayr, W. N. Hardy, D. A. Bonn, R. Liang, and H. A. Mook, Phys. Rev. Lett. **103**, 167002 (2009).

[21] W. Huang, V. Pacradouni, M. P. Kennett, S. Komiya, and J. E. Sonier, Phys. Rev. B **85**, 104527 (2012).

[22] A. Pal, K. Akintola, M. Potma, M. Ishikado, H. Eisaki, W. N. Hardy, D. A. Bonn, R. Liang, and J. E. Sonier, Phys. Rev. B **94**, 134514 (2016).

[23] S. Strässle, J. Roos, M. Mali, H. Keller, and T. Ohno, Phys. Rev. Lett. **101**, 237001 (2008).

[24] S. Strässle, B. Graneli, M. Mali, J. Roos, and H. Keller, Phys. Rev. Lett. **106**, 097003 (2011).

[25] A. M. Mounce, S. Oh, J. A. Lee, W. P. Halperin, A. P. Reyes, P. L. Kuhns, M. K. Chan, C. Dorow, L. Ji, D. Xia, X. Zhao, and M. Greven, Phys. Rev. Lett. **111**, 187003 (2013).

[26] T. Wu, H. Mayaffre, S. Krämer, M. Horvatić, C. Berthier, W. N. Hardy, R. Liang, D. A. Bonn, and M.-H. Julien, Nat. Commun. **6**, 6438 (2015).

[27] T. P. Croft, E. Blackburn, J. Kulda, Ruixing Liang, D. A. Bonn, W. N. Hardy, and S. M. Hayden, Phys. Rev. B **96**, 214504 (2017).

[28] P. Bourges, Y. Sidis, and L. Mangin-Thro, arXiv:1710.08173.

[29] S. W. Lovesey, D. D. Khayavin, and U. Staub, J. Phys.: Condens. Matter **27**, 292201 (2015).

[30] M. Fechner, M. J. A. Fierz, F. Thöle, U. Staub, and N. A. Spaldin, Phys. Rev. B **93**, 174419 (2016).

[31] J. E. Sonier, W. Huang, V. Pacradouni, M. P. Kennett, and S. Komiya, J. Phys.: Conf. Ser. **449**, 012013 (2013).

[32] J. Zhang, Z. F. Ding, C. Tan, K. Huang, O. O. Bernal, P.-C. Ho, G. D. Morris, A. D. Hillier, P. K. Biswas, S. P. Cottrell, H. Xiang, X. Yao, D. E. MacLaughlin, and L. Shu, arXiv:1703.06799.

[33] N. Nishida and H. Miyatake, Hyperfine Interact. **63**, 183 (1990).

[34] J. E. Sonier, arXiv:1706.03023.

[35] Z. Yamani, B. W. Statt, W. A. MacFarlane, R. Liang, D. A. Bonn, and W. N. Hardy, Phys. Rev. B **73**, 212506 (2006).

[36] See Supplemental Material at http://link.aps.org/supplemental/10.1103/PhysRevB.97.060502 for details on the sample growth and sample arrangement in the μSR experiments.

[37] Y. J. Uemura, in *Muon Science*, edited by S. L. Lee, S. H. Kilcoyne, and R. Cywinski (Institute of Physics, Bristol, U.K., 1999), pp. 85–114.

[38] R. S. Hayano, Y. J. Uemura, J. Imazato, N. Nishida, T. Yamazaki, and R. Kubo, Phys. Rev. B **20**, 850 (1979).

[39] I. M. Vishik, M. Hashimoto, R.-H. He, W.-S. Lee, F. Schmitt, D. Lu, R. G. Moore, C. Zhang, W. Meevasana, T. Sasagawa, S. Uchida, K. Fujita, S. Ishida, M. Ishikado, Y. Yoshida, H. Eisaki, Z. Hussain, T. P. Devereaux, and Z.-X. Shen, Proc. Natl. Acad. Sci. USA **109**, 18332 (2012).

[40] J. Crocker, A. P. Dioguardi, N. apRoberts-Warren, A. C. Shockley, H.-J. Grafe, Z. Xu, J. Wen, G. Gu, and N. J. Curro, Phys. Rev. B **84**, 224502 (2011).

[41] E. H. da Silva Neto, P. Aynajian, A. Frano, R. Comin, E. Schierle, E. Weschke, A. Gyenis, J. Wen, J. Schneeloch, Z. Xu, S. Ono, G. Gu, M. Le Tacon, and A. Yazdani, Science **343**, 393 (2014).

[42] L. Chaix, G. Ghiringhelli, Y. Y. Peng, M. Hashimoto, B. Moritz, K. Kummer, N. B. Brookes, Y. He, S. Chen, S. Ishida, Y. Yoshida, H. Eisaki, M. Salluzzo, L. Braicovich, Z.-X. Shen, T. P. Devereaux, and W.-S. Lee, Nat. Phys. **13**, 952 (2017).

[43] R. Comin and A. Damascelli, Annu. Rev. Condens. Matter Phys. **7**, 369 (2016).

[44] Y. Tanabe, T. Adashi, K. M. Suzuki, M. Akoshima, S. Heguri, T. Kawamata, Y. Ishii, T. Suzuki, I. Watanabe, and Y. Koike, J. Phys. Soc. Jpn. **83**, 074707 (2014).

[45] J. Corson, R. Mallozzi, J. Orenstein, J. N. Eckstein, and I. Bozovic, Nature (London) **398**, 221 (1999).

[46] M. S. Grbić, M. Požek, D. Paar, V. Hinkov, M. Raichle, D. Haug, B. Keimer, N. Barišić, and A. Dulčić, Phys. Rev. B **83**, 144508 (2011).

[47] L. S. Bilbro, R. Valdés Aguilar, G. Logvenov, O. Pelleg, I. Božović, and N. P. Armitage, Nat. Phys. **7**, 298 (2011).